Journal Name

COMMUNICATION

The binding modes of $V^{IV}O^{2+}$ ion in blood proteins and enzymes†

Received 00th January 20xx,
Accepted 00th January 20xx

DOI: 10.1039/x0xx00000x

www.rsc.org/

Giuseppe Sciortino,*[a,b] and Eugenio Garribba*[b]

The binding modes of $V^{IV}O^{2+}$ ion to hemoglobin (Hb), human serum transferrin (hTf), immunoglobulin G (IgG), vanadium bromoperoxidase (VBrPO) and $V^{IV}O^{2+}$-substituted imidazoleglycerol-phosphatase dehydratase (IGPD) were determined by a combined approach of full DFT and MM techniques. The results reproduce and explain the spectroscopic (EPR and ESEEM) data.

The role of free metals or metal complexes in biology and medicinal chemistry is well documented.[1] The association of metals to proteins (metalation) plays a key role in this context because it determines their transport in the bloodstream, cell uptake and, finally, influences their biological and pharmacological action.[2] Among the metals with potential applications in medicine, vanadium (V) emerged as one of the most interesting and has been proposed for the treatment of type II diabetes and various types of cancers.[3] When administered orally or with an intravenous/intraperitoneal injection, vanadium compounds in the oxidation states +IV and +V enter the bloodstream where they interact with serum proteins and erythrocytes.[4] $V^{IV}O^{2+}$ ion, bound to transferrin (hTf) at the free iron binding sites as the adducts $(V^{IV}O)$(hTf) and $(V^{IV}O)_2$(hTf) could be internalized in the cells by receptor-mediated endocytosis.[5] In the cellular environment $[V^{IV}O(OH)_3]^-$ and $[V^{V}O_2(OH)_2]^-$ ($\equiv H_2V^{V}O_4^-$) are responsible of the pharmacological effects, for example the antidiabetic action through the inhibition of protein tyrosine phosphatase.[6] However, *in vivo* blood circulation monitoring-electron spin resonance experiments with inorganic salts and complexes showed that, in rats at least 90% of V is present in the oxidation state +IV;[7] moreover, the hydrolysis at V concentration found in the organism causes the release of $V^{IV}O^{2+}$ from $V^{IV}OL_2$ potential drugs.[4] Therefore, the interaction of $V^{IV}O^{2+}$ with proteins is fundamental to: i) clarify its potential application in medicine and ii) design more active compounds taking into account a clear drug delivery strategy.

Another important application of $V^{IV}O^{2+}$ is as marker to extract specific information on the metal binding sites of peptides and proteins through electron paramagnetic resonance (EPR) when X-ray determinations (XRD) are not possible.[8]

The most relevant challenge in modelling metal–protein binding is, besides second coordination sphere interactions (*non-covalent* or *surface binding*), the treatment of coordination bond formation with accessible amino acid side-chains (*coordinative binding*), a possibility precluded with standard force-field based techniques. We recently updated the GOLD software,[9] generating a new series of parameters for the GoldScore force-field to expand its applications to the prediction of *coordinative binding*.[10,11] The approach has been validated on a dataset including more than 60 metal–protein adducts,[10,11] allowing us to reproduce in a blind manner, among others, the structure of $V^{IV}O$(picolinate)$_2$–lysozyme (Asp-COO^- donor; PDB: 4c3w[12]), $V^{V}O_3$(Benzohydroxammate)–chymotrypsin A (Ser-O^-; 2p8o[13]), $V^{V}O_4$–alkaline phosphatase (Ser-O^-; PDB: 1b8j[14]), $V^{V}O_4$–acid phosphatase (His-N; 1rpt[15]) and $V^{V}O_4$–tyrosine phosphatase (Cys-S^-; 3i80[16]).

In this communication, we used a multi-level MM and full DFT based strategy to unveil the binding modes and sites of $V^{IV}O^{2+}$ ion with important blood proteins, hemoglobin (Hb), human serum transferrin (hTf) and immunoglobulin G (IgG), and two enzymes, namely vanadium bromoperoxidase (VBrPO) and $V^{IV}O^{2+}$-substituted imidazoleglycerol-phosphatase dehydratase (IGPD). First, the proteins were probed for regions satisfying the coordination criteria suggested by EPR; second, docking assays were carried out on the identified regions; third, the predicted structures were refined at full DFT level following the cluster method proposed by Siegbahn and Himo,[17] and QM binding energy computed; finally, EPR (and, when available, electron spin echo envelope modulation, ESEEM) parameters were calculated for the predicted sites (particularly, $A_z(^{51}V)^{calcd}$) and compared with the experimental data reported up to now ($A_z(^{51}V)^{exptl}$). This step allows identifying, among the possible sites, those which reproduce the spectroscopic behaviour. The computational procedure is described in the ESI†.

[a] *Departament de Química, Universitat Autònoma de Barcelona, 08193 Cerdanyola del Vallés, Barcelona, Spain. E-mail: giuseppe.sciortino@uab.cat*
[b] *Dipartimento di Chimica e Farmacia, Università di Sassari, Via Vienna 2, I-07100 Sassari, Italy. E-mail: garribba@uniss.it*

† Electronic Supplementary Information (ESI) available: [computational procedure, tables and figures with predicted structural data and QM refined binding sites]. See DOI: 10.1039/x0xx00000x.

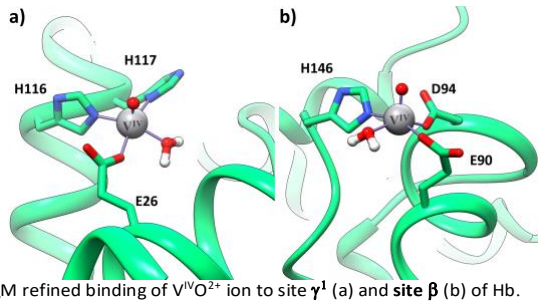

Fig. 1 QM refined binding of $V^{IV}O^{2+}$ ion to site **γ**[1] (a) and **site β** (b) of Hb.

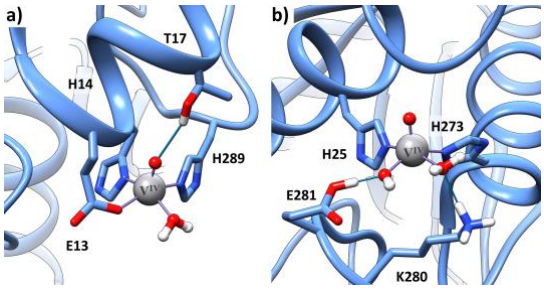

Fig. 2 QM refined binding of $V^{IV}O^{2+}$ ion to **site C** of hTf: (a) **C**[1] and (b) **C**[2].

In a first step, the method was further tested on the unique $V^{IV}O^{2+}$–adducts deposited in the PDB, with α-ketoglutarate-dependent taurine dioxygenase (PDB: 6edh[18]) and with a variant of cyt cb_{562} (PDB: 6dyl[19]). In all the cases, the binding sites were successfully predicted with a root mean square deviation (RMSD) from the experimental XRD of 0.091 and 0.039 Å (Figs. S1 and S2†), confirming the robustness of our method (further details in the ESI†).

Hb. A significant fraction of the pharmacologically active vanadium compounds is taken up by erythrocytes. This can partly or totally deactivate the specific V drug, unless it is excreted before reaching the target organs. Most of the experimental studies indicate that, inside the erythrocytes, $V^{IV}O^{2+}$ ion is bound mainly to Hb.[20,21] EPR spectra recorded in 2014 at pH 7.4 indicated that there are at least two sites, with ^{51}V hyperfine coupling constant $A_z(^{51}V)^{exptl}$ of 163.3 (**site γ**) and 166.8 × 10^{-4} cm^{-1} (**site β**), Fig. S3†.[21] On the basis of the "additivity relationship",[22] the binding of two and one His, respectively, was supposed but this information was not demonstrated. Our results suggest that Hb has two potential sites (Fig. 1 and Table 1): the first involves His116, His117 and Glu26 plus a water molecule, while the second one His146, Glu90 and Asp94. These sites can be identified with those named **γ** (two His-N bound to V^{IV}) and **β** (one His-N). For **site γ** three solutions are found (**γ**[1]-**γ**[3], Fig. S4†) with a different position of the V=O bond with respect to the donors and high values of GoldScore *Fitness* (F_{max} and F_{mean}) and population (Table S1†). QM refinement of the two sites predicts bond distances in line with those expected (Table S2†).[23] The computed $\Delta E_{binding}$ values for the formation of the three sites indicate that the stability of the sites **β** and **γ** is comparable, in agreement with the similar intensity of their EPR signals; furthermore, the order of $A_z(^{51}V)$ is: **site γ** < **site β**, coherent with the experimental data (Fig. S3†).

hTf. The main function of transferrin is the transport of iron in the organism. It binds reversibly two Fe^{3+} ions in the *N*- and *C*-terminal sites (hTf_N and hTf_C).[5] In normal plasma, only 30% of transferrin binds Fe^{3+} (corresponding to a concentration of available sites of ca. 50 μM) and other metal ions can occupy hTf_N and hTf_C, i.e. Bi^{3+}, Al^{3+}, Ru^{3+}, Cu^{2+}, Mn^{2+}, Zn^{2+}, Ni^{2+}, and vanadium in its three oxidation states (+III, +IV, and +V).[24] Before 2013, it was believed that $V^{IV}O^{2+}$ binds only to hTf_N and hTf_C sites,[25] but then it was demonstrated by EPR that it can interact also with iron-saturated protein Fe_2-hTf (holo-hTf); the site was named **C** and is characterized by $A_z(^{51}V)^{exptl}$ = 165.4 × 10^{-4} cm^{-1}, measured in ref. [26] (Fig. S5†). Based on the "additivity relationship",[22] the binding of two His plus Asp/Glu-COO is plausible. For this site, the docking assay suggests three putative modes (**C**[1]-**C**[3] in Table 1 and Fig. S6†), two of them involving the coordination of two histidines, with values of *F* and population rather high, particularly for **C**[1] (His14, His289, Glu13; H_2O). The $\Delta E_{binding}$ are all negative and similar to Hb; moreover the calculated, $A_z(^{51}V)^{calcd}$, are comparable with the experimental one. All the sites are stabilized by hydrogen bond networks, particularly between V=O and Thr17-OH for **C**[1] and water molecules with Lys280-NH_3 and Glu281-COO^- for **C**[2]; this latter could favor the deprotonation of the coordinated H_2O (Fig. 2). Notably, the structure of **site C**[1] is similar to $V^{IV}O^{2+}$-substituted carboxypeptidase (coordination of His69, His196, Glu72[27]) and the values of $A_z(^{51}V)^{exptl}$ are comparable (165.9 × 10^{-4} cm^{-1} for $V^{IV}O^{2+}$–carboxypeptidase and 165.4 × 10^{-4} for hTf). The $\Delta E_{binding}$ values suggest that the **site C** could be strong enough to be considered an additional site, besides hTf_N and hTf_C, for the transport of $V^{IV}O^{2+}$ and, notably, it could be occupied even in the presence of Fe^{3+} and other metal ions. The bond lengths are shown in Table S2†.

IgG. IgG is a "Y" shaped protein (ca. 150 kDa) that represents 75% of the total immunoglobulins in the blood with a mean concentration in the range 80-90 μM.[28] Therefore, it can contribute with transferrin and albumin to the transport of $V^{IV}O^{2+}$ in the organism. Despite an interaction with Cu^{2+}, Mn^{2+}, and Ru^{2+} was substantiated in the literature, the binding to $V^{IV}O^{2+}$ was only recently demonstrated.[29] Some years ago EPR spectra were measured and suggested that at pH 7.4 $V^{IV}O^{2+}$ ion distributes on at least three distinct coordination environments with $A_z(^{51}V)^{exptl}$ of 158.8 × 10^{-4} cm^{-1} (**site 1**), 163.6 × 10^{-4} cm^{-1} (**site 2**) and 167.4 × 10^{-4} cm^{-1} (**site 3**), Fig. S7†.[29] A decreasing donor strength from **site 1** to **3**, which would result in an increase of $A_z(^{51}V)$, is expected. The low $A_z(^{51}V)$ for **site 1** suggests the possible presence of a strong donor, such as Tyr-O^-, Ser/Thr-O^- or Cys-S^-. Ser and Thr residues are exposed on the protein surface, particularly in the fragment antigen binding region (Fab, located on the arms of the "Y") and their number is much higher than Tyr and Cys.[30]

Preliminary docking analysis allows finding four potential sites with at least three donors (Table 1, Table S1† and Fig. S8†). The interface C_H1/CL region of the Fab domain with Asn138, Asp167, Asp170, His172, and Ser174 is particularly interesting and can bind $V^{IV}O^{2+}$ with three or four amino acid side-chains. The values of F_{max}, F_{mean} and populations are very high, the $\Delta E_{binding}$ always negative and $A_z(^{51}V)^{calcd}$ can be compared with the experimental values of **sites 1** and **2**. **Site 2** could be based on the coordinative binding of NCO group of Asp170 plus His172 of another chain, with Ser174 (and Thr172) engaged in a hydrogen bond with V=O (Fig. 3b). Upon deprotonation of Ser174 a rearrangement occurs with alcoholate-O^- of serine

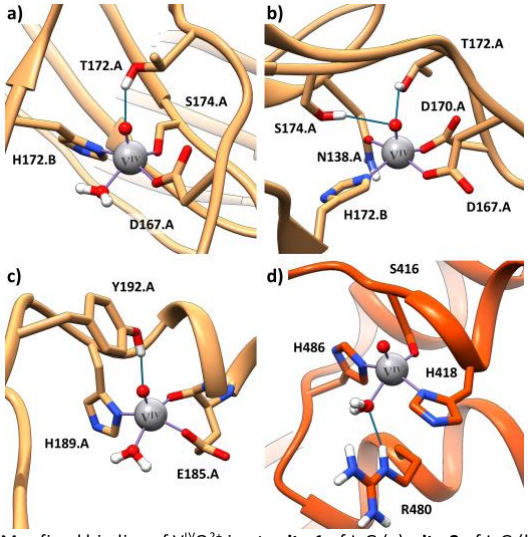

Fig. 3 QM refined binding of $V^{IV}O^{2+}$ ion to **site 1** of IgG (a), **site 2** of IgG (b), **site 3**[1] of IgG (c) and to VBrPO (d).

that replaces Asp170-COO^- with formation of **site 1** (Fig. 3a). So, at pH 7.4 the two **sites 1** and **2** are in equilibrium and both populated. The **site 3** could be one of the two solutions with coordination of one His-N, one Glu-COO^- and Asp/Glu-CO, plus a water molecule in the fourth equatorial position found at the C_L chain of the Fab or at the C_H3 of the Fc region, the base of the "Y" that plays a role in modulating immune cell activity (Fig. 3c).

VBrPO. VBrPO is a metalloenzyme containing a mononuclear V^V co-factor that catalyses the oxidation of halides in the presence of hydrogen peroxide.[6] The first example of a VBrPO was isolated from the marine alga *A. nodosum*; the XRD revealed in the active site a trigonal bipyramidal V^V atom with only one His residue (His418) bound to metal.[6] Upon reduction to V^{IV} by dithionite, the enzyme was irreversibly inactivated but can be easily studied by EPR spectroscopy. The measurement of EPR spectra dates back 1988 (Fig. S9†): $A_z(^{51}V)^{exptl}$ value is 167.5 × 10^{-4} cm^{-1} at pH 4.2 and 160.1 × 10^{-4} cm^{-1} at pH 8.4.[31] Experimental modulation frequencies, arising from Δm_I = ±1 transitions, of 3.1 and 5.3 MHz were observed in the ESEEM spectrum and assigned to His residues in the equatorial plane.[32] The results of the docking study (Table 1, Table S2† and Fig. S10†) indicate only one solution with F_{max} and F_{mean} higher than 50. All the 50 docking poses were found in this cluster: $V^{IV}O^{2+}$ ion is bound by three different donors, the deprotonated Ser416, and His418 and His486 in *trans* position (Fig. 3d). This means that, in the reduced form, Ser416 and His 486 add to His418 bound to V in the native form. The values of $A_z(^{51}V)^{calcd}$ (156.0 × 10^{-4} cm^{-1}) and $A_{iso}(^{14}N)^{calcd}$ (2.3 and 5.3 MHz) are in good agreement with the experiment.[31-32] The alternative binding mode, with Ser416-OH protonated and deprotonation of H_2O induced by Arg480[34], was also explored. The values of $\Delta E_{binding}$ and $A_z(^{51}V)^{calcd}$ (165.0 × 10^{-4} cm^{-1}) are comparable with the first mode (Table 1); however, the $A_{iso}(^{14}N)^{calcd}$ (6.9 and 7.3 MHz) significantly differ from the experimental values making the coordination mode (Ser416-O^- ; H_2O) the most probable candidate.

Overall, EPR data as a function of pH can be rationalized postulating that at low pH Ser and His are partially protonated giving the large value of $A_z(^{51}V)^{exptl}$, while at high pH their deprotonation results in the formation of the site presented in Fig. 3d, causing the lowering of $A_z(^{51}V)$.

$V^{IV}O^{2+}$-substituted IGPD. IGPD is a Mn^{II}-dependent enzyme involved in the biosynthesis of histidine which catalyses the dehydration of imidazole glycerol phosphate to imidazole acetol phosphate.[35] The binding of $V^{IV}O^{2+}$ to the inactive *apo*-protein was used to explore the metal environment.[33] The X-band EPR spectrum $V^{IV}O^{2+}$-substituted IGPD from *S. cerevisiae* was recorded Petersen *et al*. (Fig. S11†) and showed at physiological pH the resonances of three different sites (denoted **α**, **β**, and **γ**), indicating different coordination environments, with $A_z(^{51}V)^{exptl}$ of 169.1 × 10^{-4} cm^{-1} (**α**), 161.6 × 10^{-4} cm^{-1} (**β**) and 140.6 × 10^{-4} cm^{-1} (**γ**), probably in equilibrium between each other.[33] The values of $A_z(^{51}V)^{exptl}$ for **sites α** and **β** would suggest the binding of His residues and $A_{iso}(^{14}N)^{exptl}$ = 7.0 MHz measured by ESEEM confirms this insight.[33]

The docking results indicate four possible solutions with comparable scoring and population, distributed in three sites (Table 1, Table S1† and Fig. S12†). In the **sites α** and **β** three histidines and a glutamate take part to the coordination. $A_z(^{51}V)^{calcd}$ and $A_{iso}(^{14}N)^{calcd}$ (6.1-6.9 MHz for site **α** and 6.3-7.0 MHz for **β**) are coherent with the experimental data. For the

Table 1 Binding modes of serum proteins and enzymes for $V^{IV}O^{2+}$ ion identified by docking, binding energies and $A_z(^{51}V)$ constants computed on their full QM optimized structures.

Protein	Donors	F_{max}[a]	F_{mean}[b]	Pop.[c]	$\Delta E_{binding}$[d]	$A_z(^{51}V)^{calcd}$[e]	$A_z(^{51}V)^{exptl}$[e]
Hb	N_{H146}, COO^-_{E90}, COO^-_{D94}; H_2O (**site β**)[f]	40.2	37.8	3	-30.9	171.2	166.8 [g]
Hb	N_{H116}, N_{H117}, COO^-_{E26}; H_2O (**site γ**[1])[f]	61.3	55.8	22	-29.2	168.7	163.3 [g]
hTf	N_{H14}, N_{H289}, COO^-_{E13}; H_2O (**site C**[1])[f]	66.0	59.0	27	-24.3	169.5	165.4 [h]
hTf	N_{H25}, N_{H273}; H_2O, OH^- (**site C**[2])[f,i]	38.8	38.8	37	-32.8	167.9	165.4 [h]
hTf	N_{H473}, COO^-_{D478}; H_2O, H_2O (**site C**[3])[f,j]	37.6	34.7	12	-26.4	168.6	165.4 [h]
IgG	N_{H172}, COO^-_{D167}, O^-_{S174}; H_2O (**site 1**)[f]	75.0	69.3	47	-19.5	158.4	158.8 [k]
IgG	N_{H172}, COO^-_{D167}, COO^-_{D170}, NCO_{N138} (**site 2**)[f]	57.8	55.2	48	-31.8	165.8	163.6 [k]
IgG	N_{H189}, COO^-_{E185}, CO_{E185}; H_2O (**site 3**[1])[f]	52.5	46.5	42	-26.2	171.0	167.4 [k]
IgG	N_{H460}, COO^-_{E461}, CO_{D399}; H_2O (**site 3**[2])[f]	42.4	37.7	45	-23.5	172.3	167.4 [k]
VBrPO	N_{H418}, N_{H486}, O^-_{S416}; H_2O (**mode 1**)[f]	66.3	65.4	50	-8.0	156.0	160.1 [l]
VBrPO	N_{H418}, N_{H486}, OH_{S416}; OH^- (**mode 2**)[f]	56.3	55.4	50	-11.6	165.0	160.1 [l]
IGPD	N_{H47}, N_{H74}, N_{H169}, COO^-_{E173} (**site α**[1])[f]	54.9	52.2	16	-43.1	166.8	169.1 [m]
IGPD	N_{H73}, N_{H145}(ax), N_{H170},COO^-_{E77}; H_2O (**site β**)[f]	52.9	50.0	8	-47.4	164.3	161.6 [m]
IGPD	N_{H113}, N_{H159}, O^-_{S115}; H_2O[f]	47.9	47.1	2	-15.3	156.0	140.6 [m]

[a] GoldScore *Fitness* value obtained for the more stable pose of each *cluster*. [b] Average value of GoldScore *Fitness* for each *cluster*. [c] Population of the *cluster*. [d] $\Delta E_{binding}$ in kcal/mol. [e] $A_z(^{51}V)$ reported in 10^{-4} cm^{-1} units as absolute values. [f] Other possible binding modes are summarized in Table S1 and Figs. S3-S7 of the ESI†. [g] Ref. [21]. [h] Ref. [26]. [i] *cis* arrangement of H_2O and OH^- ligands. [j] *trans* arrangement of H_2O ligands. [k] Ref. [29]. [l] Ref. [31]. [m] Ref. [33].

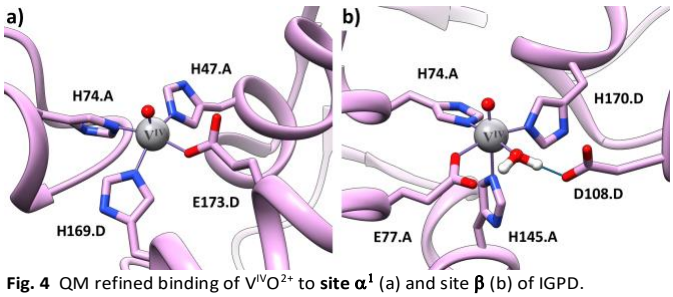

Fig. 4 QM refined binding of $V^{IV}O^{2+}$ to **site α¹** (a) and site **β** (b) of IGPD.

site α two binding modes were obtained, the first (site **α¹**, Fig. 4a) with His74, His47, His170, Glu173 on the equatorial plane ($A_z(^{51}V)^{calcd}$ = 166.8 × 10^{-4} cm^{-1}), the second with His169 in the axial position in *trans* to V=O ($A_z(^{51}V)^{calcd}$ = 164.9 × 10^{-4} cm^{-1}, Table S1†). An axial histidine (His145) is predicted also for the interdomain **site β** (Fig. 4b). The resonance below 2.5 MHz in the ESEEM spectrum could confirm this finding ($A_{iso}(^{14}N)^{calcd}$ are 0.5 and 0.5 MHz for the **sites α** and **β**). These results are coherent with the sites determined for Mn^{II} ions.[35] Finally, the last site found, with (His113, His159, Ser115; H_2O), has the lowest $\Delta E_{binding}$ and cannot account for the unusually low experimental value of 140.6 × 10^{-4} cm^{-1} for **site γ**, that – therefore – remains unassigned.

In summary, we characterized at molecular level the binding modes of $V^{IV}O^{2+}$, which is one of the active species released from V drugs at physiological conditions, with blood proteins and two V enzymes. The validity of the obtained results has been verified through the comparison of the DFT simulated and experimental spectroscopic data. The donors with high affinity are His-N and Asp/Glu-COO^-, but the binding of deprotonated Ser residues is possible. This approach has a general applicability to any metals and proteins, and could give new insights on the transport and mechanism of action of metal-based drugs and be helpful for the design of more active compounds accounting for a rational drug delivery strategy.

E.G. and G.S. thank Regione Autonoma della Sardegna (grant RASSR79857), Università di Sassari (fondo di Ateneo per la ricerca 2020) and Spanish MINECO (CTQ2017-87889-P) for the financial support.

Conflicts of interest

There are no conflicts to declare.

Notes and References

1. (a) N. P. E. Barry and P. J. Sadler, *Chem. Commun.*, 2013, **49**, 5106; (b) K. D. Mjos and C. Orvig, *Chem. Rev.*, 2014, **114**, 4540.
2. (a) A. Merlino, T. Marzo and L. Messori, *Chem.–Eur. J.*, 2017, **23**, 6942; (b) D. Loreto, G. Ferraro and A. Merlino, *Int. J. Biol. Macromol.*, 2020, **163**, 970.
3. (a) J. Costa Pessoa, S. Etcheverry and D. Gambino, *Coord. Chem. Rev.*, 2015, **301-302**, 24; (b) D. Rehder, *Future Med. Chem.*, 2016, **8**, 325; (c) D. C. Crans, L. Henry, G. Cardiff and B. I. Posner, in *Essential Metals in Medicine: Therapeutic Use and Toxicity of Metal Ions in the Clinic*, ed. P. L. Carver, De Gruyter GmbH, Berlin, 2019, pp. 203.
4. T. Jakusch and T. Kiss, *Coord. Chem. Rev.*, 2017, **351**, 118.
5. R. Crichton, *Iron Metabolism - From Molecular Mechanisms to Clinical Consequences*, John Wiley & Sons, Ltd, Chichester, 2009.
6. (a) D. C. Crans, J. J. Smee, E. Gaidamauskas and L. Yang, *Chem. Rev.*, 2004, **104**, 849; (b) D. Rehder, *Bioinorganic Vanadium Chemistry*, John Wiley & Sons, Ltd, Chichester, 2008.
7. H. Yasui, K. Takechi and H. Sakurai, *J. Inorg. Biochem.*, 2000, **78**, 185.
8. D. N. Chasteen, in *Met. Ions Biol. Syst.*, eds. H. Sigel and A. Sigel, Marcel Dekker, New York, 1995, vol. 31, pp. 231.
9. G. Jones, P. Willett, R. C. Glen, A. R. Leach and R. Taylor, *J. Mol. Biol.*, 1997, **267**, 727.
10. (a) G. Sciortino, J. Rodríguez-Guerra Pedregal, A. Lledós, E. Garribba and J.-D. Maréchal, *J. Comput. Chem.*, 2018, **39**, 42; (b) G. Sciortino, E. Garribba and J.-D. Maréchal, *Inorg. Chem.*, 2019, **58**, 294.
11. G. Sciortino, D. Sanna, V. Ugone, G. Micera, A. Lledós, J.-D. Maréchal and E. Garribba, *Inorg. Chem.*, 2017, **56**, 12938.
12. M. F. A. Santos, I. Correia, A. R. Oliveira, E. Garribba, J. Costa Pessoa and T. Santos-Silva, *Eur. J. Inorg. Chem.*, 2014, 3293.
13. A. Moulin, J. H. Bell, R. F. Pratt and D. Ringe, *Biochemistry*, 2007, **46**, 5982.
14. K. M. Holtz, B. Stec and E. R. Kantrowitz, *J. Biol. Chem.*, 1999, **274**, 8351.
15. Y. Lindqvist, G. Schneider and P. Vihko, *Eur. J. Biochem.*, 1994, **221**, 139.
16. T. A. S. Brandão, A. C. Hengge and S. J. Johnson, *J. Biol. Chem.*, 2010, **285**, 15874.
17. P. E. M. Siegbahn and F. Himo, *Wiley Interdiscip. Rev. Comput. Mol. Sci.*, 2011, **1**, 323.
18. K. M. Davis, M. Altmyer, R. J. Martinie, I. Schaperdoth, C. Krebs, J. M. Bollinger and A. K. Boal, *Biochemistry*, 2019, **58**, 4218.
19. J. Rittle, M. J. Field, M. T. Green and F. A. Tezcan, *Nature Chem.*, 2019, **11**, 434.
20. I. G. Macara, K. Kustin and L. C. Cantley Jr, *Biochim. Biophys. Acta, Gen. Subj.*, 1980, **629**, 95.
21. D. Sanna, M. Serra, G. Micera and E. Garribba, *Inorg. Chem.*, 2014, **53**, 1449.
22. (a) D. N. Chasteen, in *Biological Magnetic Resonance*, eds. L. J. J. Berliner and J. Reuben, Plenum Press, New York, 1981, vol. 3, pp. 53; (b) T. S. Smith II, R. LoBrutto and V. L. Pecoraro, *Coord. Chem. Rev.*, 2002, **228**, 1.
23. L. F. Vilas Boas and J. Costa Pessoa, in *Comprehensive Coordination Chemistry*, eds. G. Wilkinson, R. D. Gillard and J. A. McCleverty, Pergamon Press, Oxford, 1985, vol. 3, pp. 453.
24. H. Sun, M. Cox, H. Li and P. Sadler, *Struct. Bonding*, 1997, **88**, 71.
25. J. Costa Pessoa, E. Garribba, M. F. A. Santos and T. Santos-Silva, *Coord. Chem. Rev.*, 2015, **301–302**, 49.
26. D. Sanna, G. Micera and E. Garribba, *Inorg. Chem.*, 2013, **52**, 11975.
27. R. J. DeKoch, D. J. West, J. C. Cannon and N. D. Chasteen, *Biochemistry*, 1974, **13**, 4347.
28. R. G. Hamilton, *Clin. Chem.* , 1987, **33**, 1707.
29. D. Sanna, G. Micera and E. Garribba, *Inorg. Chem.*, 2011, **50**, 3717 and references therein.
30. S. Nishihara, A. Shimizu and Y. Arata, *Mol. Immunol.*, 1986, **23**, 285.
31. E. De Boer, K. Boon and R. Wever, *Biochemistry*, 1988, **27**, 1629.
32. E. de Boer, C. P. Keijzers, A. A. K. Klaassen, E. J. Reijerse, D. Collison, C. D. Garner and R. Wever, *FEBS Lett.*, 1988, **235**, 93.
33. J. Petersen, T. R. Hawkes and D. J. Lowe, *J. Inorg. Biochem.*, 2000, **80**, 161 and references therein.
34. T. S. Smith II, C. A. Root, J. W. Kampf, P. G. Rasmussen and V. L. Pecoraro, *J. Am. Chem. Soc.*, 2000, **122**, 767.
35. C. Bisson, K. L. Britton, S. E. Sedelnikova, H. F. Rodgers, T. C. Eadsforth, R. C. Viner, T. R. Hawkes, P. J. Baker and D. W. Rice, *Structure*, 2015, **23**, 1236.

